Supplementary Material

Cobalt Nanoparticle-Encapsulated N-Doped Carbon Nanotubes on 3D Porous Carbon: A Novel Platform for Ultrasensitive Electrochemical Sensing of Rutin

Zhewei Zhang[a, b], Zijian Zhao[a,b,*], Yaqi Yang[a,b,*]

[a] *College of Pharmacy, Shaanxi University of Chinese Medicine, Xianyang 712000, People's Republic of China*

[b] *College of Chemistry and Materials Engineering, Huaihua University, Huaihua 418000, People's Republic of China*

** Yaqi Yang, Ph.D., College of Chemistry and Materials Engineering, Huaihua University, HuaiHua, China*

E-mail: yyq880@126.com

** Zijian Zhao, Ph.D., College of Chemistry and Materials Engineering, Huaihua University, HuaiHua, China*

E-mail: zjzhao72@163.com

Tables

Table S1: Comparison of various electrochemical methods for rutin detection

Electrode	Linear range (μM)	LOD (nM)	Ref.
CdTeQD-MMXene/GCE	0.099-653.6	0.033	[1]
NF/AuNPs/N-CPDs@FLBP/SPE	0.001-10	0.033	[2]
ZIF-8@MWCNTs/CP	0.01-190	2.82	[3]
PCN-224@ARC	0.05-1	11.7	[4]
C-GCS@ZIF-F/PL	0.1-100	5.4	[5]
$Ti_3Al_{0.5}Cu_{0.5}C_2$MAX	0.05-50	15	[6]
FeCo@C	0.01-2	3.41	[7]
Co@N-CNTs/3DHC	0.0001-0.05, 0.05-1	0.0415	This work

Table S2. The detection results of rutin from actual samples of buckwheat tea and rutin tablets (n=3)

Samples	Added (nM)	Found (nM)	Recovery (%)	RSD (%)	Condetermined by UV-Vis spectroscopy(diluted)
Buckwheat tea		39.22±1.1		2.9	39.66 nM
	20	59.36±0.7	100.7	1.2	
	40	77.98±0.08	96.9	0.1	
	100	138.26±1.4	99.04	1	
Rutin tables		39.34±1.6		4	39.8 nM
	20	59.15±0.8	99.05	1.4	
	40	78.79±1.3	98.6	1.7	
	100	142.44±2.1	103.1	1.5	

Figures

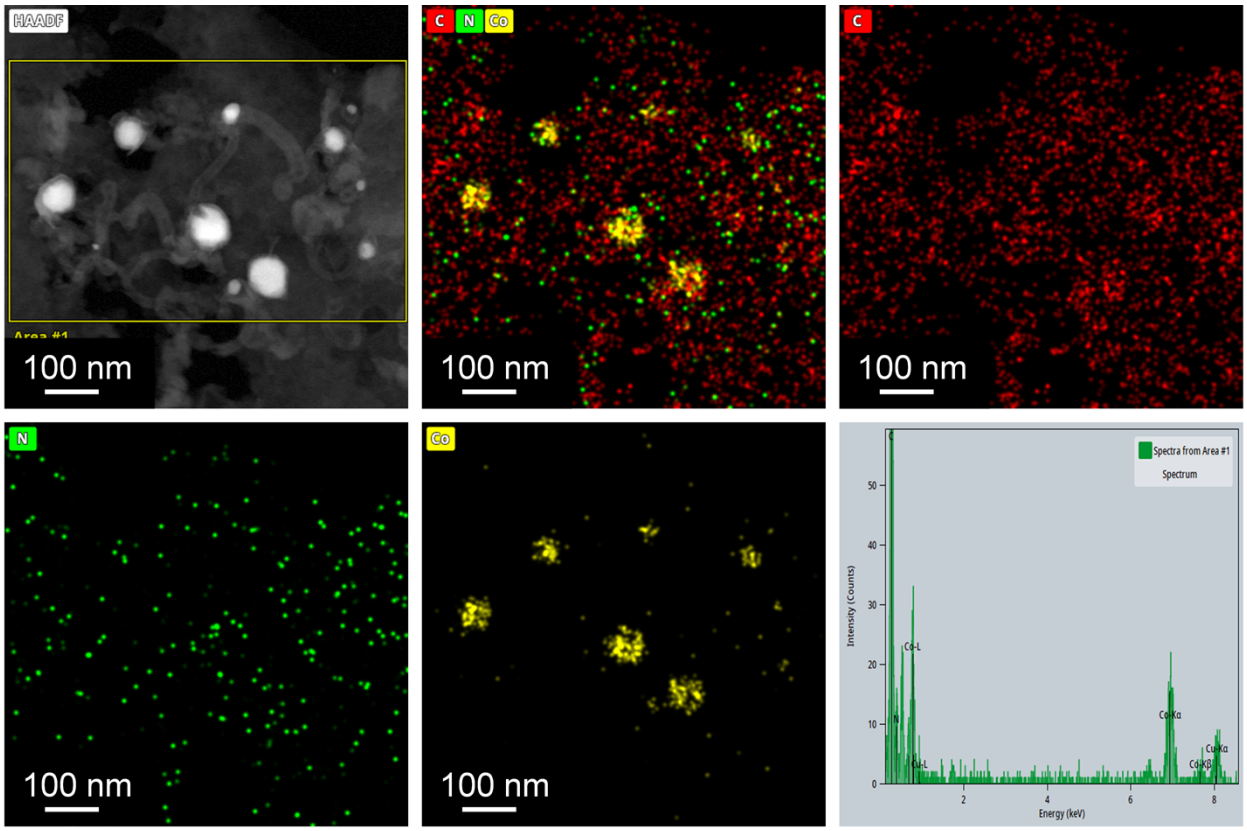

Fig. S1. TEM and element mapping images of Co@N-CNTs/3DHC (C, N, Co).

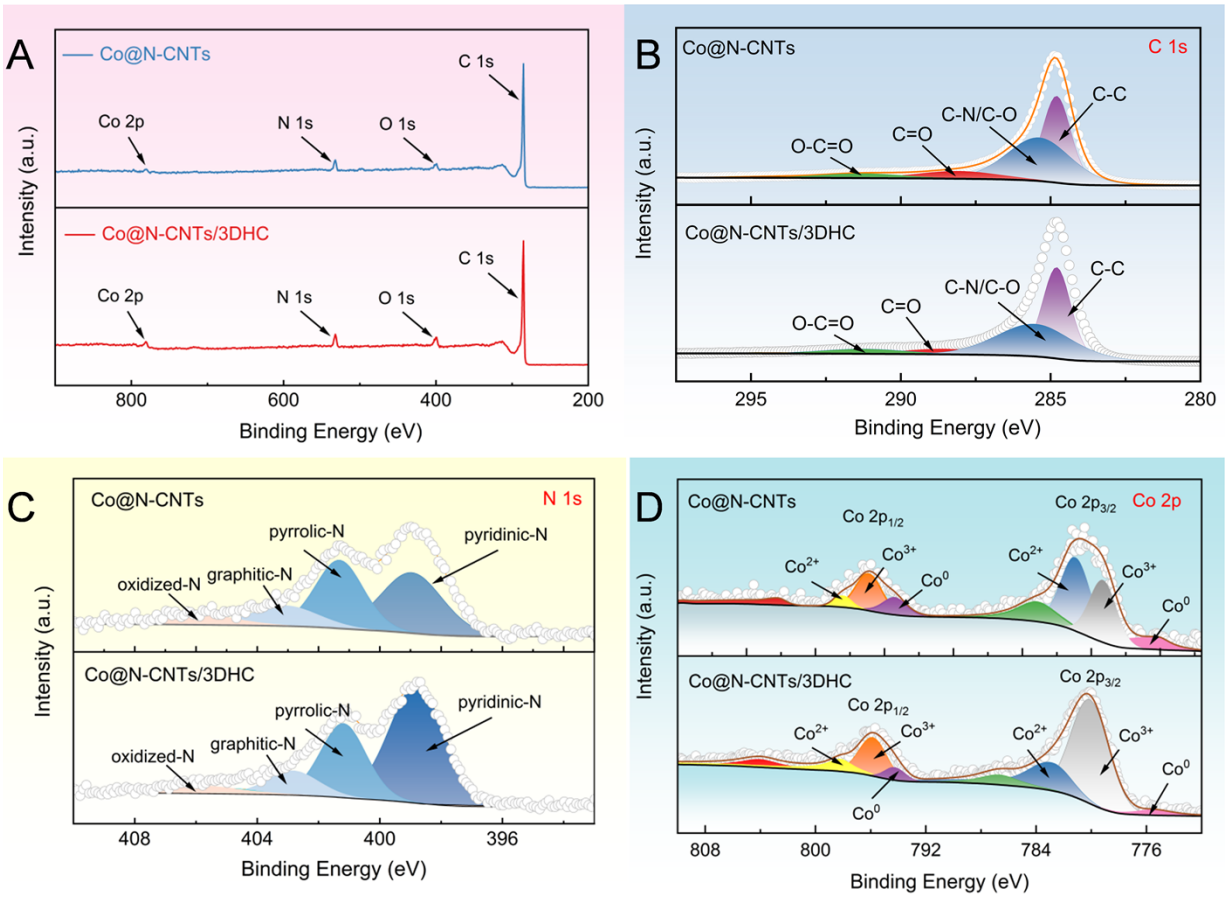

Fig. S2. (A) XPS spectra of Co@N-CNTs and Co@N-CNTs/3DHC; High-resolution XPS spectra of C 1s (B), N 1s (C), and Co 2p (D) in the related composite materials.

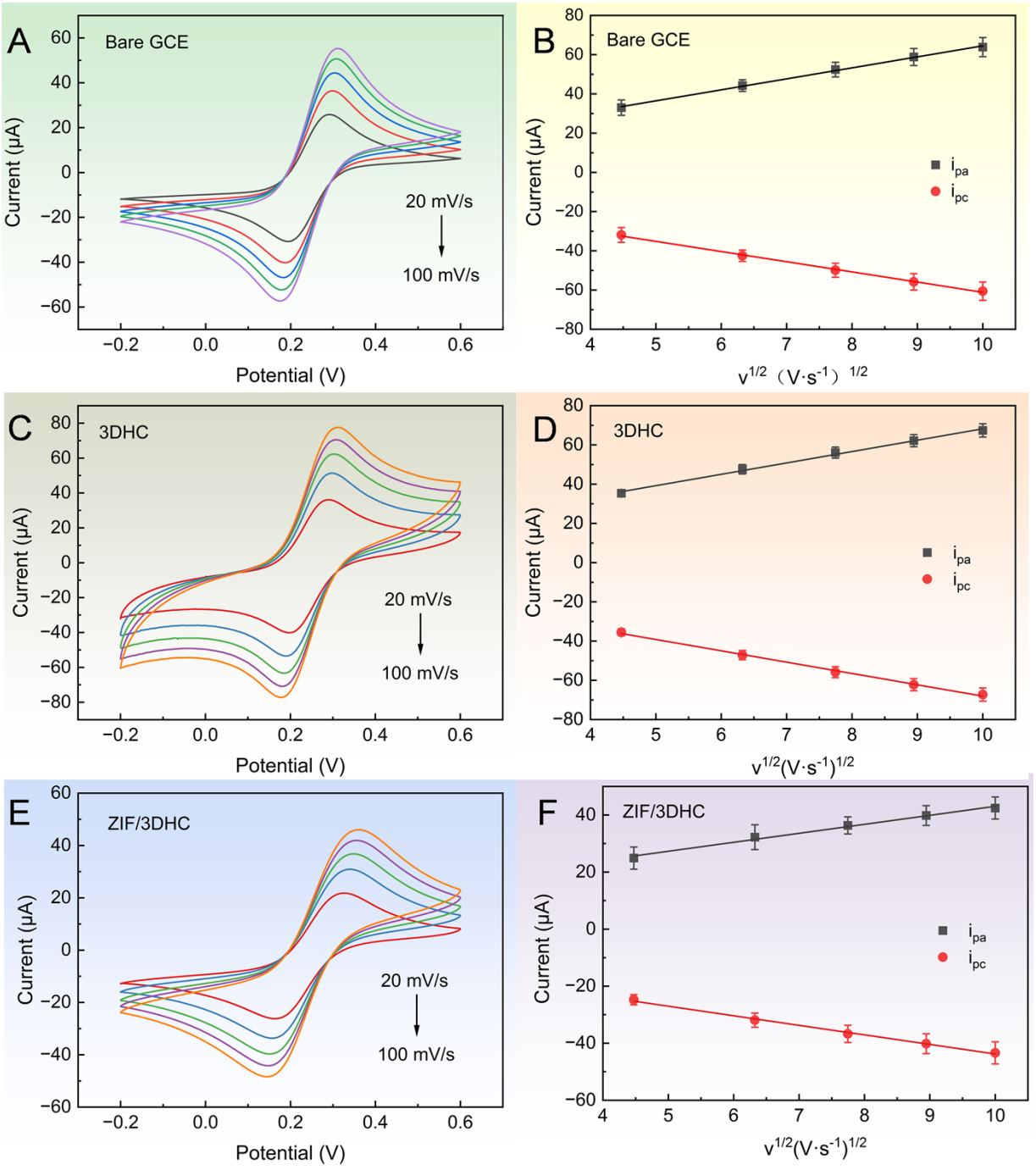

Fig. S3. In a 0.1M KCl solution containing 5×10^{-3} M $[Fe(CN)_6]^{3-}$, (A) Bare GCE, (C) 3DHC and (E) ZIFs/3DHC show CV curves under different scan rates (20, 40, 60, 80, 100, 120, 140, 180, 200, 220, 240, 260, 280, 300); (B) Bare GCE, (D) 3DHC and (F) ZIFs/3DHC's oxidation and reduction peak currents have a linear relationship with the scan rate.

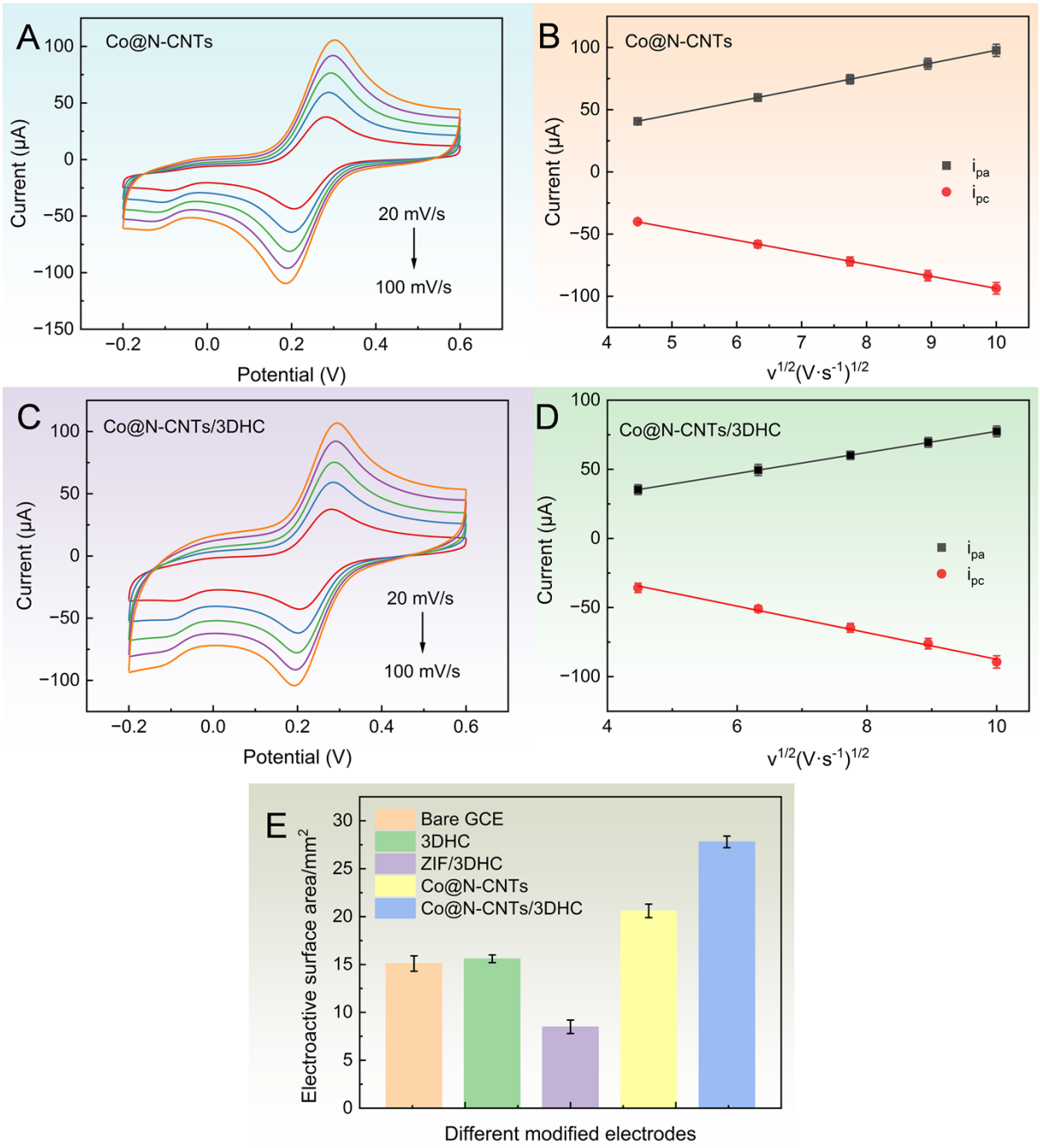

Fig. S4. In a 0.1M KCl solution with a 5×10^{-3} M $[Fe(CN)_6]^{3-}$ concentration, (A) Co@N-CNTs and (C) Co@N-CNTs/3DHC show their CV curves under different scan rates (20, 40, 60, 80, 100, 120, 140, 180, 200, 220, 240, 260, 280, 300); (B) the linear relationship between the oxidation and reduction peak currents of Co@N-CNTs and Co@N-CNTs/3DHC and the scan rate; (E) the comparison of the specific surface areas of different modified electrodes.

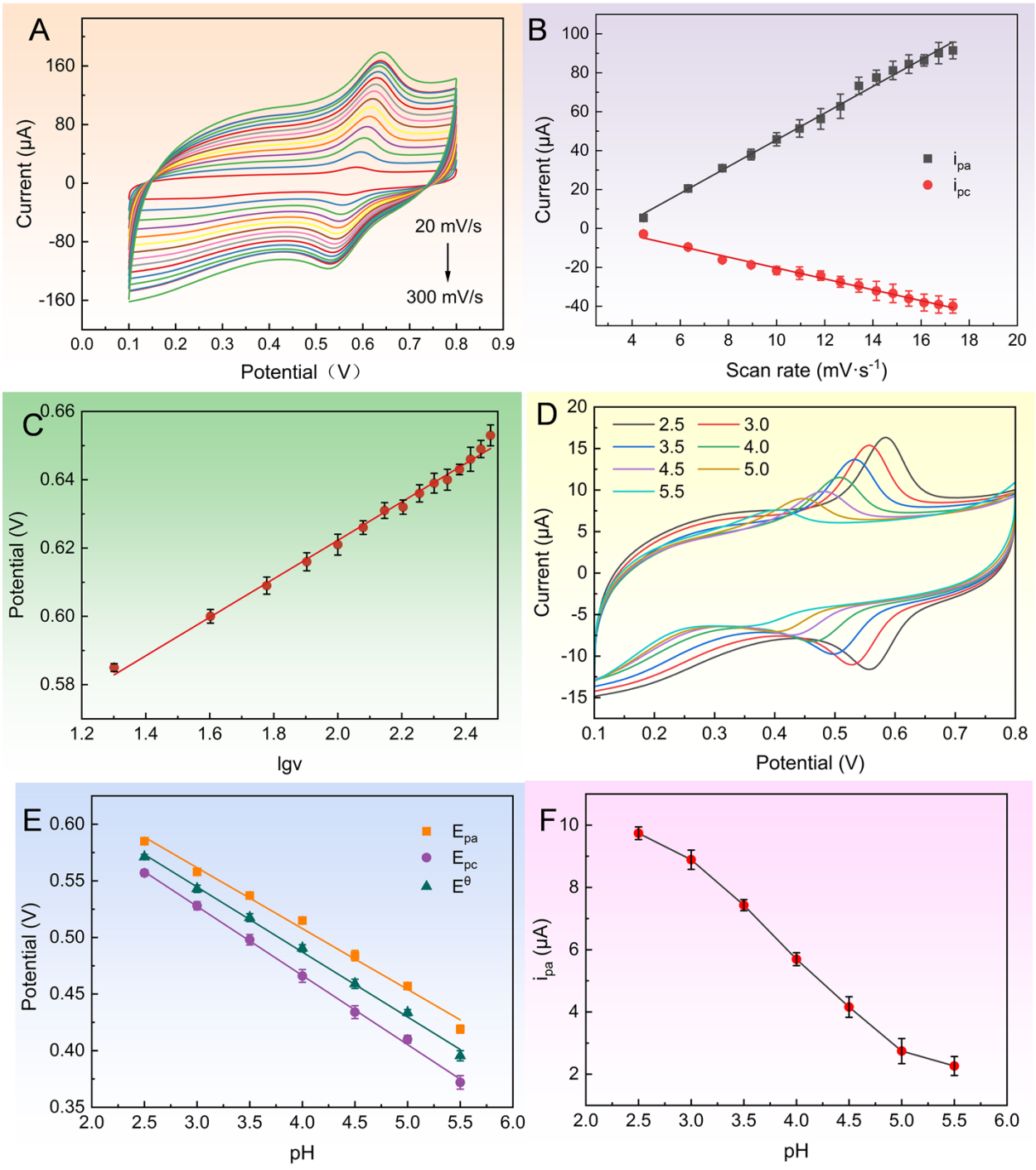

Fig. S5. (A) CV curves of Co@N-CNTs/3DHC under different scan rates (20, 40, 60, 80, 100, 120, 140, 180, 200, 220, 240, 260, 280, 300) at 1 μM rutin concentration; (B) Linear relationship between scan rate and oxidation and reduction peak currents; (C) Corresponding relationship between logarithm of peak current and logarithm of scan rate; (D) Cyclic voltammograms of Co@N-CNTs/3DHC for 1 μM rutin at different pH

values (2.5, 3.0, 4.5, 5.0, 5.5, 6.0, 6.5); (E) Linear relationship diagram between pH value and oxidation-reduction potential; (F) Linear relationship diagram between pH value and peak current.

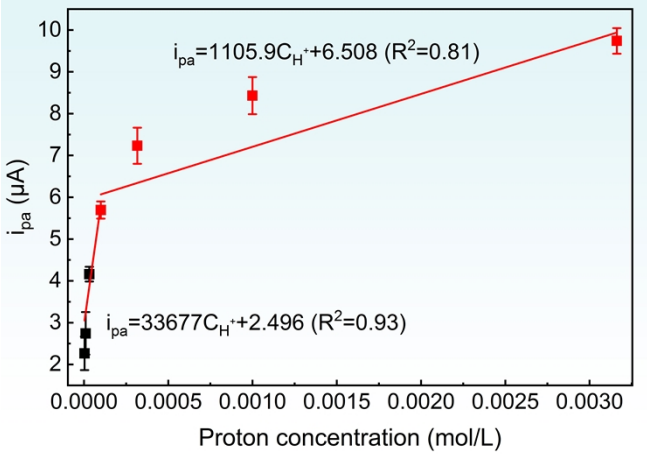

Fig. S6. Relationship between the anodic peak current (i_{pa}) and proton concentration ([H^+]) for rutin oxidation at the Co@N-CNTs/3DHC electrode.

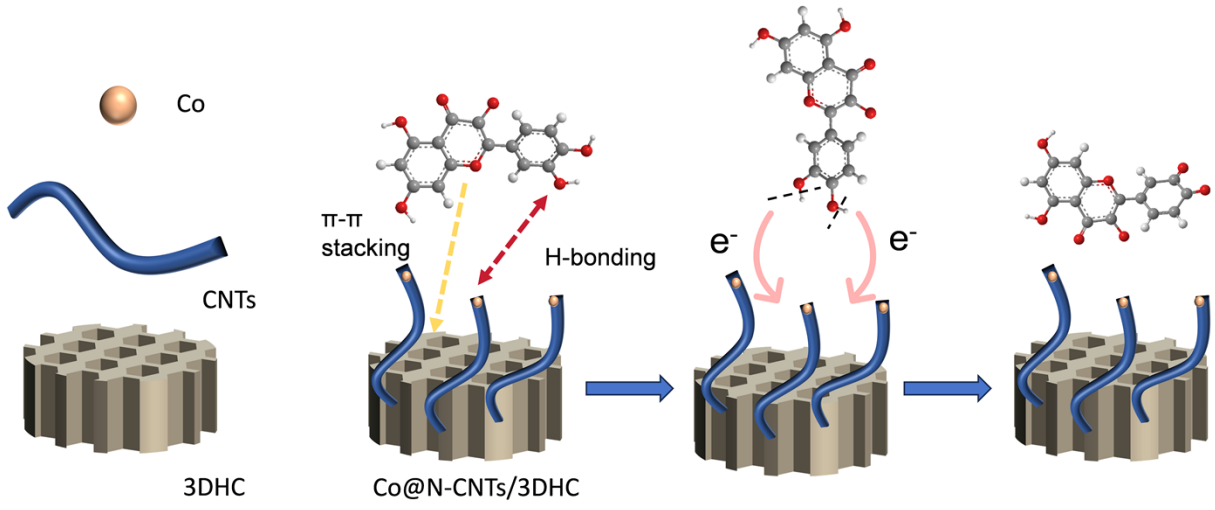

Fig. S7. Proposed reaction mechanism of rutin at the surface of Co@N-CNTs/3DHC/GCE.

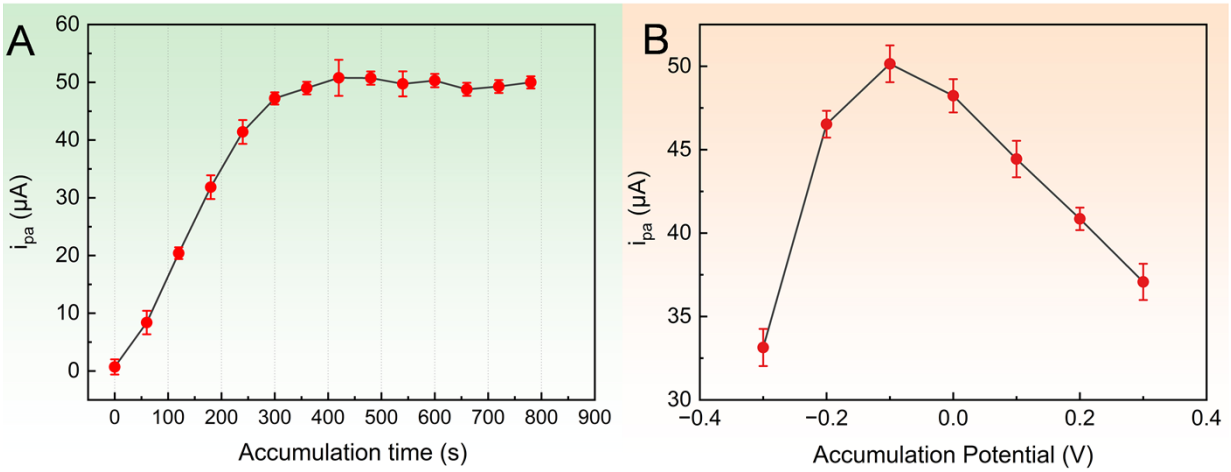

Fig. S8. (A) Graph showing the variation of peak current with enrichment time; (B) Graph showing the variation of peak current with enrichment potential.

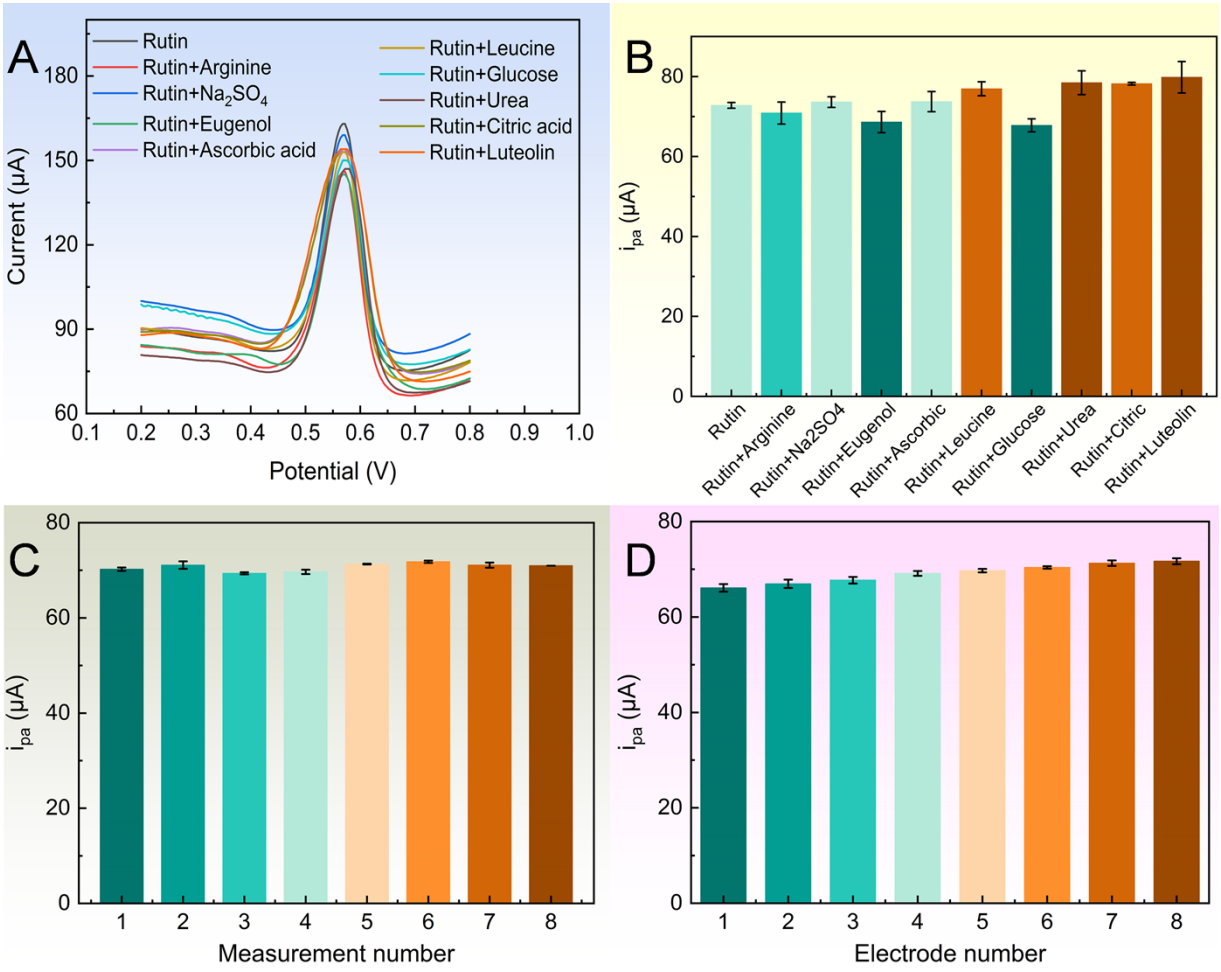

Fig. S9. (A) DPV of Rt on Co@N-CNTs/3DHC when various interfering substances are added; (B) Comparison of signals before and after adding interfering substances during Rt detection; (C) DPV signal obtained by repeating 8 times in 1 μM rutin; (D) DPV signals obtained from 8 different electrodes in 1μM.

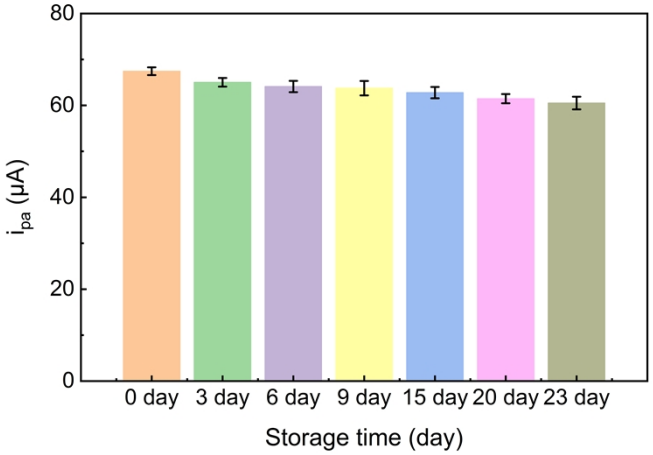

Fig.S10. Long-term stability test of the Co@N-CNTs/3DHC/GCE sensor.

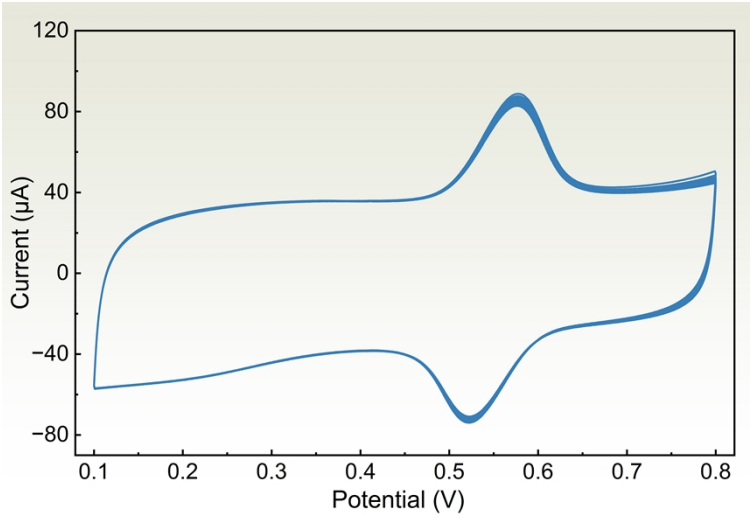

Fig.S11. Repeated cyclic voltammograms (15 consecutive cycles) of the Co@N-CNTs/3DHC/GCE.

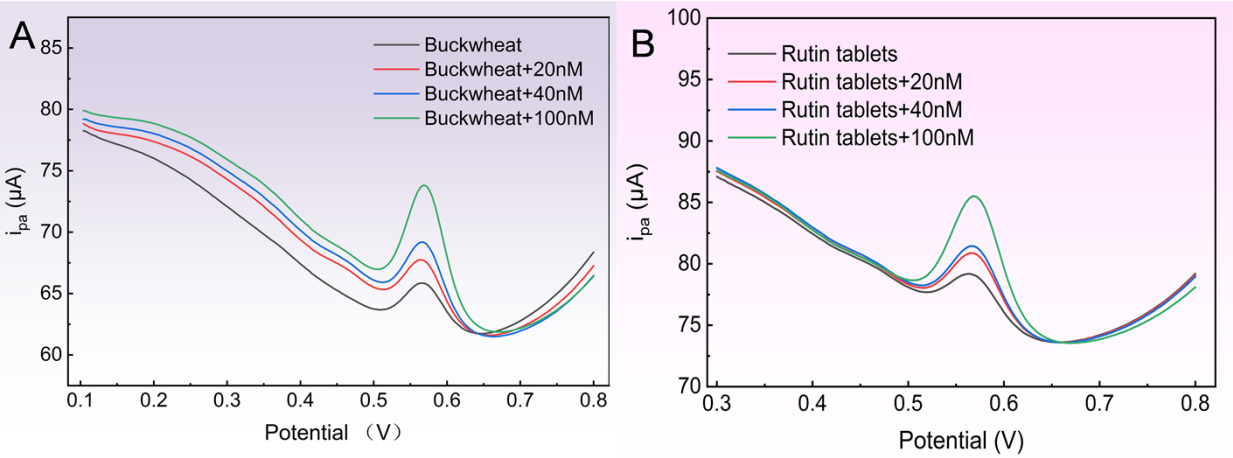

Fig.S12. Recovery test of rutin in real samples using the standard addition method. (A) DPV curves for a buckwheat extract. (B) DPV curves for a commercial rutin tablet sample.

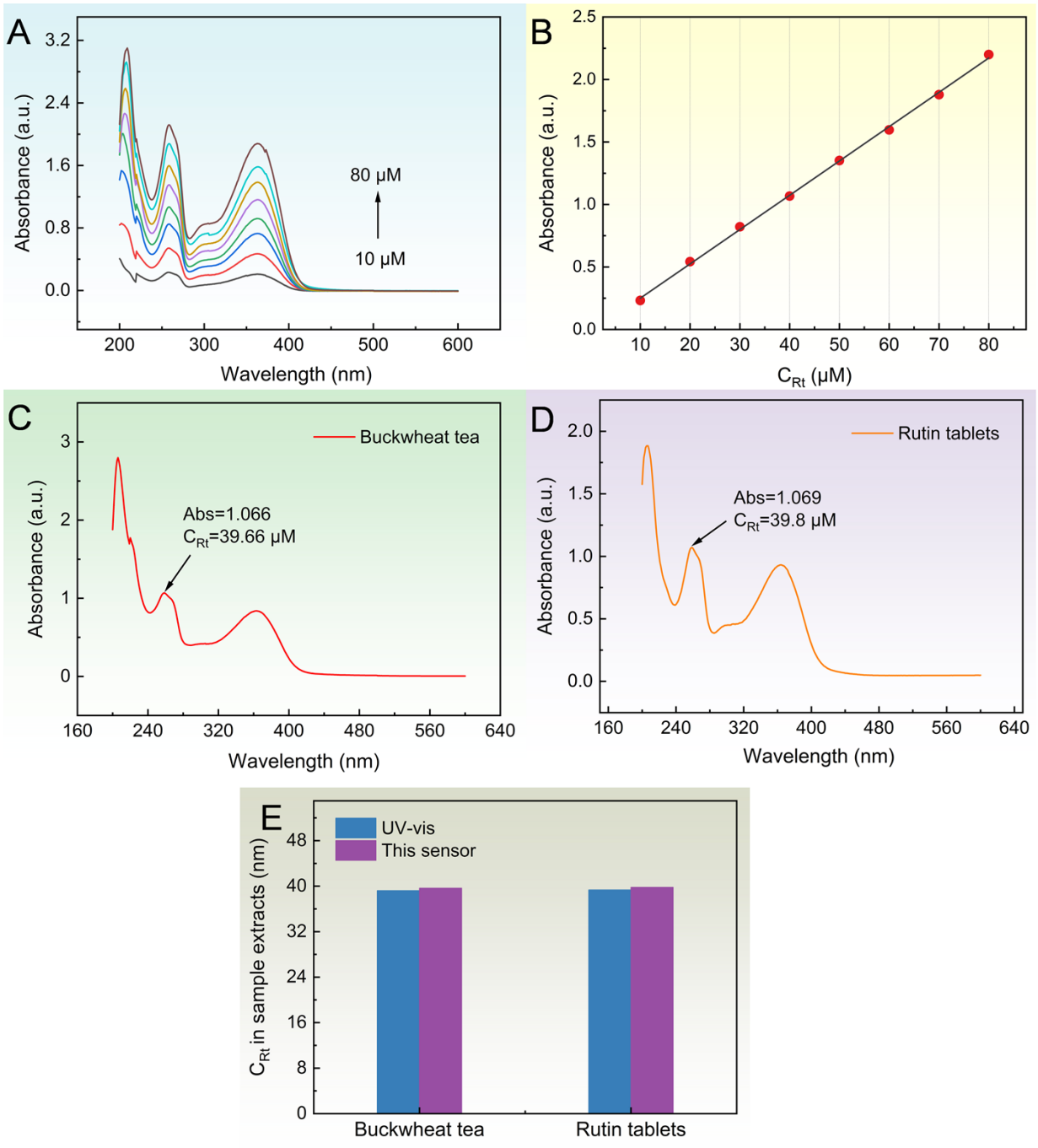

Fig. S13. (A) Ultraviolet-visible spectrum of the rutin standard solution; (B) Linear calibration curve of the rutin standard solution; (C) Ultraviolet-visible spectrum of the rutin tablet; (D) Ultraviolet-visible spectrum of the ethanol extract of tartary buckwheat; (E) Comparison of the detection of rutin in actual sample extracts by Co@N-CNTs/3DHC.

[1] L. Li, L. Liu, J. Zhou, C. Gu, X. Wu, C. Lei, L. Yan, Cadmium telluride quantum dot-MXene composite–based electrochemical sensing platform for simultaneous determination of rutin and quercetin in foods, Microchimica Acta 192(4) (2025) 238.
[2] F. Shi, Y. Ai, B. Wang, Y. Yao, Z. Zhang, J. Zhou, X. Wang, W. Sun, Portable Wireless Intelligent Electrochemical Sensor for the Ultrasensitive Detection of Rutin Using Functionalized Black Phosphorene Nanocomposite, Molecules, 2022.
[3] X. Ma, W. Pang, Y. Gao, X. Chang, Z. Hu, T. Hu, A Paper-Based Electrochemical Sensor Based on Chain Structured ZIF-8@MWCNTs for Efficient Determination of Rutin, Journal of The Electrochemical Society 171(4) (2024) 047514.
[4] C. Liu, H.-Y. Du, C. Xin, X. Di, Synthesis of porphyrin-based metal-organic framework and biomass-derived carbon composite for electrochemical detection of Rutin, Journal of Electroanalytical Chemistry 984 (2025) 119058.
[5] K. Yang, F. Han, Y. Jin, X. Li, C-GCS@ZIF-F/PL based electrochemical sensor for rapid and ultra-sensitive detection of rutin in foods, Food Chemistry 460 (2024) 140382.
[6] A. Şenocak, V. Sanko, S.O. Tümay, Y. Orooji, E. Demirbas, Y. Yoon, A. Khataee, Ultrasensitive electrochemical sensor for detection of rutin antioxidant by layered Ti3Al0.5Cu0.5C2 MAX phase, Food and Chemical Toxicology 164 (2022) 113016.
[7] H. Gu, X. Shui, Y. Zhang, T. Zeng, J. Yang, Z. Wu, X. Zhang, N. Yang, Porous carbon scaffolded Fe-based alloy nanoparticles for electrochemical quantification of acetaminophen and rutin, Carbon 221 (2024) 118954.